Paste 2024 – AB Fourie & D Reid (eds)

doi:10.36487/ACG_repo/2455_27

Inferring the state parameter from partially drained cone penetration test data using the soil behaviour-type index to adjust drained/undrained correlations

J Ayala *Klohn Crippen Berger, Australia*

AB Fourie *The University of Western Australia, Australia*

D Reid *The University of Western Australia, Australia*

M Jefferies *Consultant, UK*

Abstract

Estimating the in situ state parameter (ψ) of mine tailings is crucial when evaluating susceptibility to liquefaction. This is usually done from cone penetration test (CPT) data. However, CPTs in partially drained conditions, which are common in mine tailings, do not have an established methodology of interpretation as yet. A simplification of the characteristic surface approach is developed to provide a method for estimating ψ which can be easily implemented in a spreadsheet. This simplified method avoids enforced use of state estimates based on fully drained or undrained CPT correlations, which can lead to incorrect dilative or contractive material state characterisations.

This simplified version of the characteristic surface method is based on using the soil behaviour-type index to infer the drainage conditions, allowing inference of ψ continuously from fully drained to fully undrained CPT responses. This approach improves the understanding of the differing effects of state and drainage over the CPT record.

Keywords: *cone penetration test, partial drainage, state parameter, soil behaviour-type index, characteristic surface*

1 Introduction

In recent years, different technologies have emerged to thicken tailings before deposition in tailings storage facilities (TSFs), making the common assumption that these partially saturated materials at deposition cannot undergo undrained shearing due to the lack of proper saturation. Understanding that thickened tailings are not deposited in a dry manner, and that the moisture present in the ensuing raise depositions may percolate into the underlying thickened tailings layers, is something that needs to be assessed by geotechnical engineers, as unsaturated conditions may not always apply. Moreover, the assumption that paste thickened tailings cannot undergo liquefaction because of the densified deposition in comparison to slurries also merits assessment as this densified deposition still does not necessarily ensure state parameters (ψ) with dilative response to shearing. Recent cone penetration test (CPT) data of paste thickened tailings on a mining site in Australia tends to fall within the silty sand to sandy silt, and the clayey silts to silty clay soil behaviour-type, with varied CPT pore pressure responses for the same deposit. Moreover, CPT data of a European paste thickened tailings show saturation and contractive states for the complete profile from about a metre from surface with varied soil behaviour-type index (I_c) values.

This work presents a method based on I_c to infer the ψ from standard CPT data, when in the drained-undrained variable region. In addition, it is shown that this method can be extended to other soils when two characteristic drainage responses are observed.

2 Background

2.1 Normalised tip resistance and the state parameter

Correlations between the tip resistance of the CPT and ψ have been documented in the literature since Been et al. (1986), with many additional contributions over the ensuing decades (Shuttle & Jefferies 1998, 2016; Been & Jefferies 1992; Shuttle & Cunning 2007; Ghafghazi & Shuttle 2008; Jefferies & Been 2015; Reid 2015; Ayala et al. 2020, 2022). Throughout, the main concept has remained the same, which is to use an exponential equation to correlate the normalised tip resistance with ψ, as shown in Equation 1:

$$Q\left(1-B_q\right)+1 = k\, e^{\,(-m\times\psi)} \tag{1}$$

where:

- $Q(1-B_q)+1$ = normalisation of the CPT tip resistance by vertical effective stress as suggested by Houlsby (1988)
- k = constant of the equation that represents the intercept at ψ = 0
- m = constant of the equation that represents the slope of the exponential correlation
- ψ = initial state parameter (this is before pushing the cone).

However, it is worth noting that Equation 1 needs to be inverted to infer the ψ from $Q(1-B_q)+1$ as initially intended. This inverted form is presented in Equation 2:

$$\psi = \frac{-\ln\left(\frac{Q(1-B_q)+1}{k}\right)}{m} \tag{2}$$

Additionally, it is important to note that a drained soil's response to the CPT advance will register a different tip resistance compared with the same soil under undrained conditions, assuming the soil ψ is far from its drained-undrained crossover point, that as shown in Figure 1 is where both drainage behaviours are similar. There are therefore two different correlations, shown with the black lines in Figure 1, implying that two sets of k and m constants, introduced in Equation 1, will be needed. These are denoted as k_{dr} and m_{dr} for the drained correlation, and k_{un} and m_{un} for the undrained correlation.

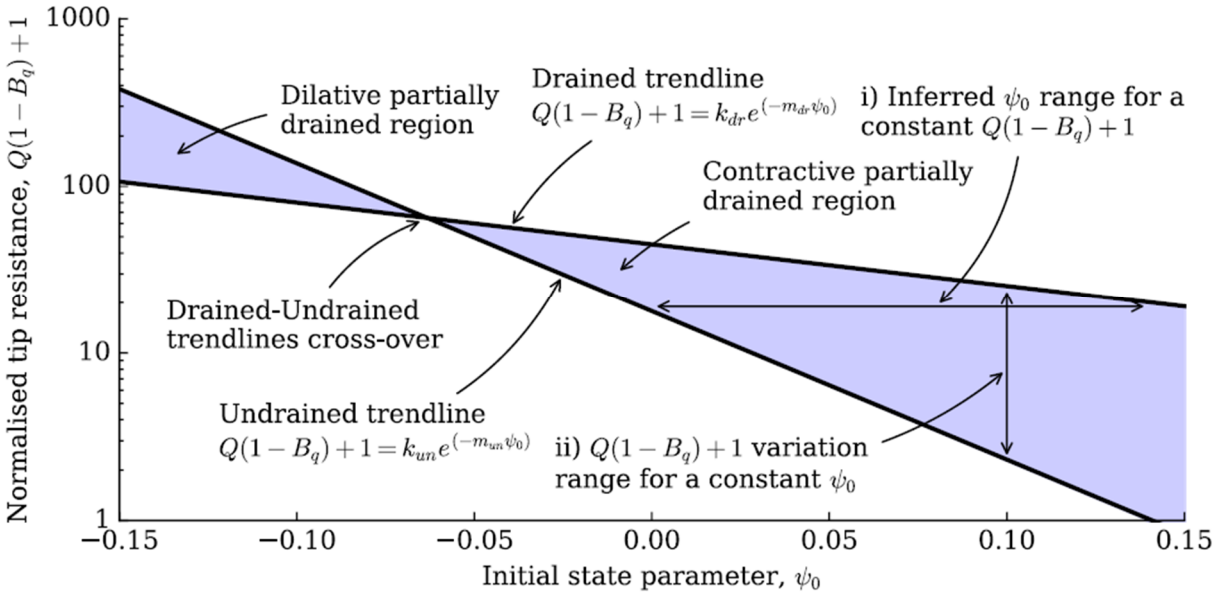

Figure 1 Standard drained and undrained correlations between the normalised tip resistance and the initial state parameter, also showing the wide range for partially drained behaviour in the contractive and dilative regions

The drained and undrained correlations cross-over, as shown in Figure 1, because contractive materials will generate positive excess pore pressures when shearing, reducing the effective stress in the material, while dilative materials will generate negative excess pore pressures, producing the opposite effect. Additionally, in Figure 1 there are two shaded regions. These correspond to partially drained responses in between fully drained and undrained regimes. The right shaded side is the contractive partially drained response region, while the left side is the dilative partially drained response region. These regions are separated by the previously mentioned drained-undrained trendlines crossover. Furthermore, label 'i' in Figure 1 shows the wide variation in possible ψ interpretations between fully drained and undrained responses, while label 'ii' shows the wide possible $Q(1-B_q)+1$ interpretation variation for a constant and known ψ, this latter case corresponding mainly to laboratory studies when the soil ψ is usually known.

Considering the case of the silty tailings shown in Figure 1, for a recorded $Q(1-Bq)+1 \approx 20$, the ψ interpretation of the soil could vary between ~0.0 and 0.14, depending on the engineer's assumption of drained or undrained conditions for the sounding, representing a significant difference when assessing the stability of TSFs. This highlights the importance of including drainage conditions in the CPT interpretation method to infer ψ.

2.2 Normalised penetration velocity and the characteristic curves for partially drained penetrations

Not accounting for partial drainage can add large uncertainties to the in situ soil state interpretation, somewhat addressed in research contributions in the past decades (House et al. 2001; Randolph & Hope 2004; Silva & Bolton 2005; Lehane et al. 2009; Jaeger et al. 2010; Low et al. 2011; Yi et al. 2012; DeJong & Randolph 2012; Mahmoodzadeh et al. 2014; Mahmoodzadeh & Randolph 2014; Suzuki & Lehane 2015; Dienstmann et al. 2018; Reid & Fourie 2018). The contribution by Finnie & Randolph (1994), being perhaps the most notable by introducing the normalised penetration velocity, shown in Equation 3, presents a standardised non-dimensional form to normalise penetration data of different soils with different testing conditions:

$$V = \frac{d \times v}{c_{hv}} \tag{3}$$

where:

- V = normalised penetration velocity
- d = cone diameter
- v = penetration rate
- c_{hv} = coefficient of consolidation for the horizontal or vertical direction, whichever is higher, usually being the horizontal direction for horizontally layered soil deposits as in TSFs.

DeJong & Randolph (2012) subsequently introduced the characteristic curve equation, allowing the penetration drainage regime to be inferred depending on knowledge of V. In their work, they validated their concept with contractive data (part of the data shown in Figure 2c) and introduced a method to infer the coefficient of consolidation from CPT dissipation test data under partially drained conditions. However, this requires knowledge or assumption, in per cent, of the extent of excess pore pressure response, driven by the CPT advance, at the start of the partially drained dissipation test, in relation to fully undrained testing conditions. Their work allowed the normalisation of different data sets such as those listed previously.

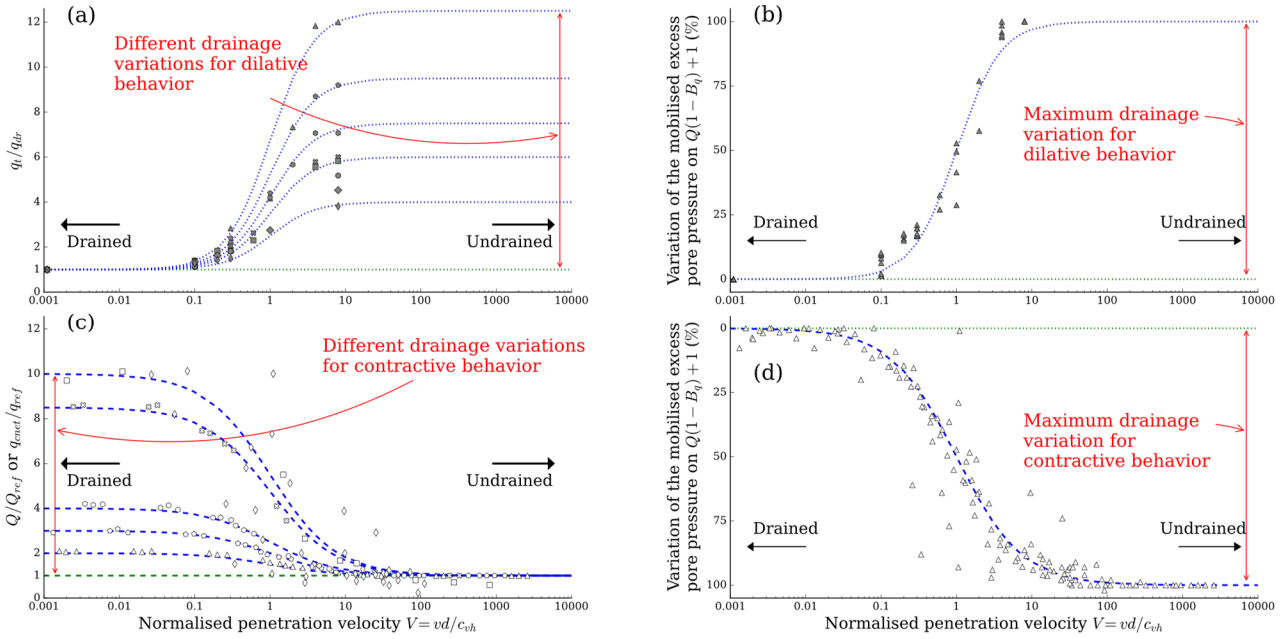

Figure 2 Different characteristic curves for (a) Dilative literature data; (b) Dilative literature data with percentage normalisation; (c) Contractive literature data; (d) Contractive literature data with percentage normalisation

Figure 2c shows the fit of various characteristic curves to data from different researchers in blue; details of which can be found in Ayala (2022). Additionally, DeJong & Randolph's (2012) work allowed Ayala et al. (2023) to slightly modify the characteristic curve concept for dilative literature data, as shown in Figure 2a. Moreover, after some additional modifications to normalise the penetration drainage variation to percentage terms, making drained penetration 0% and undrained penetration 100%, it was possible to approximate a single characteristic curve for the data. For the scattered dilative data in Figure 2a, the percentage representation is as shown in Figure 2b with an approximate single characteristic curve. For the scattered contractive data in Figure 2c, the percentage representation is shown in Figure 2d with its approximate single characteristic curve. Details of these modifications can be found in Appendix H of Ayala (2022).

2.3 Characteristic surface concept

Aiming to infer the ψ from CPT data using the method introduced by Been et al. (1986) from CPT data under partially drained conditions using the method proposed by DeJong & Randolph (2012), Ayala et al. (2023) introduced the characteristic surface concept, as shown in Figure 3, where the axes of this surface are Q(1-Bq)+1, ψ and V. However, similar to DeJong & Randolph (2012), to infer the ψ from Q(1-Bq)+1, the characteristic surface equation (Equation 4) also relies on the user knowing or assuming a percentage of the mobilised excess pore pressure during penetration (for V), which can be a limitation depending on the material and available information.

$$Q\left(1-B_q\right)+1=\frac{\left(k_{un}\,e^{\,(-m_{un}\times\psi)}-k_{dr}\,e^{\,(-m_{dr}\times\psi)}\right)}{1+(V_{50}/V)^c}+k_{dr}\,e^{\,(-m_{dr}\times\psi)} \quad (4)$$

where:

k_{dr} = constant that represents the intercept at ψ = 0 for drained penetration

m_{dr} = constant that represents the slope of the exponential correlation for drained penetration

k_{un} = constant that represents the intercept at ψ = 0 for undrained penetration

m_{un} = constant that represents the slope of the exponential correlation for undrained penetration

V_{50} = normalised penetration velocity at which one-half of the partially drained effect is mobilised

c = maximum rate of change in drainage regime with V.

Ayala et al. (2023) also introduced a two-dimensional representation of the characteristic surface that allows estimation of ψ from partially drained penetrations with the ψ-isolines. However, this also relies on the user knowing or assuming a percentage of the mobilised excess pore pressure during penetration, as explained.

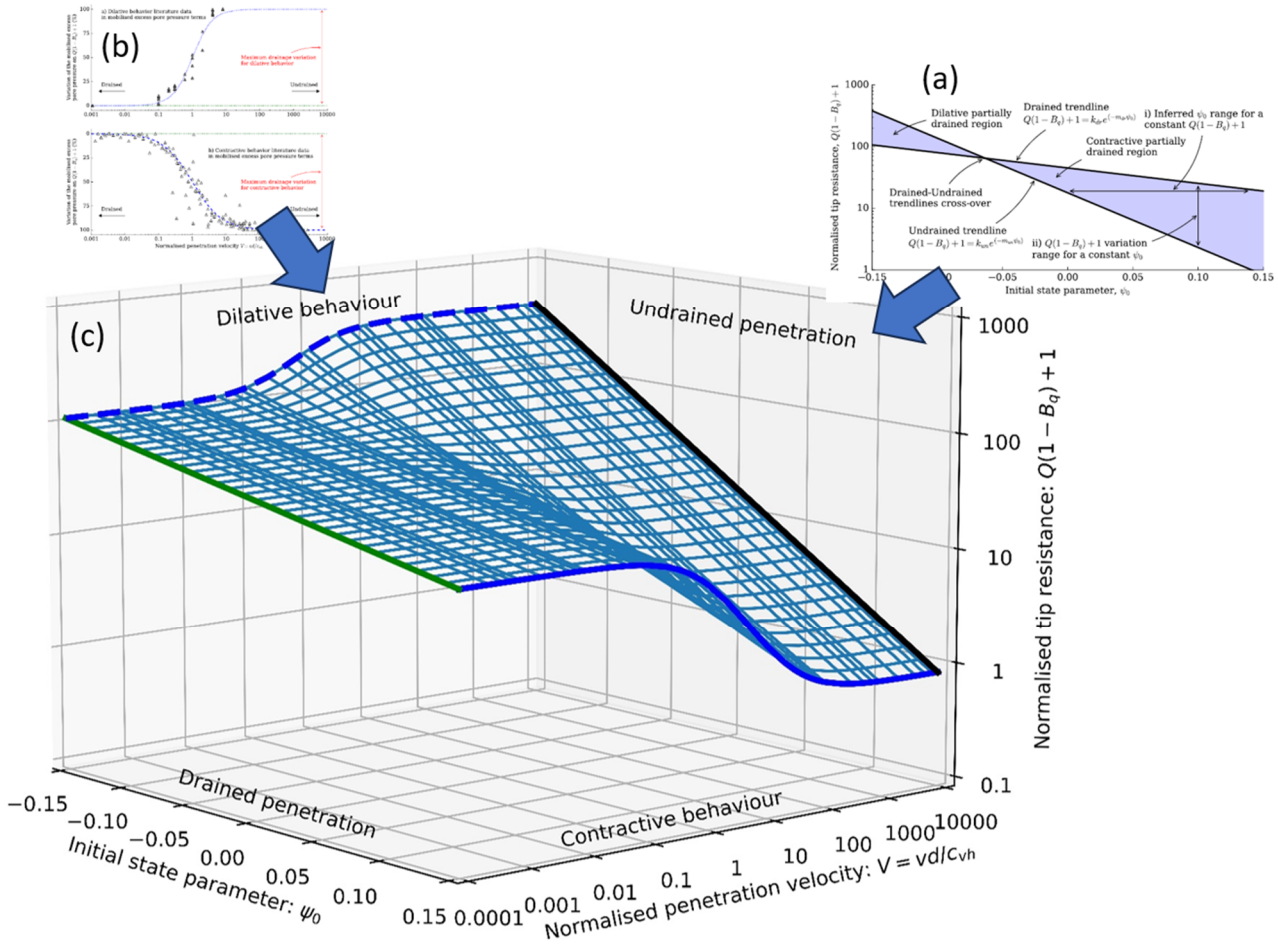

Figure 3 Unification of (a) the standard drained-undrained correlations between the normalised tip resistance and the initial state parameter, with (b) the percentage normalisation of the contractive-dilative characteristic curves with the normalised penetration velocity, to create (c) the characteristic surface

3 Soil behaviour-type index as an alternative to the normalised penetration velocity

The 'soil behaviour-type' index I_c is commonly used to infer the soil type from the normalised CPT data, as shown in Figure 4, where I_c described in Equation 5, has the soil type limits introduced by Shuttle & Cunning (2008), with further details presented by Jefferies & Been (2015).

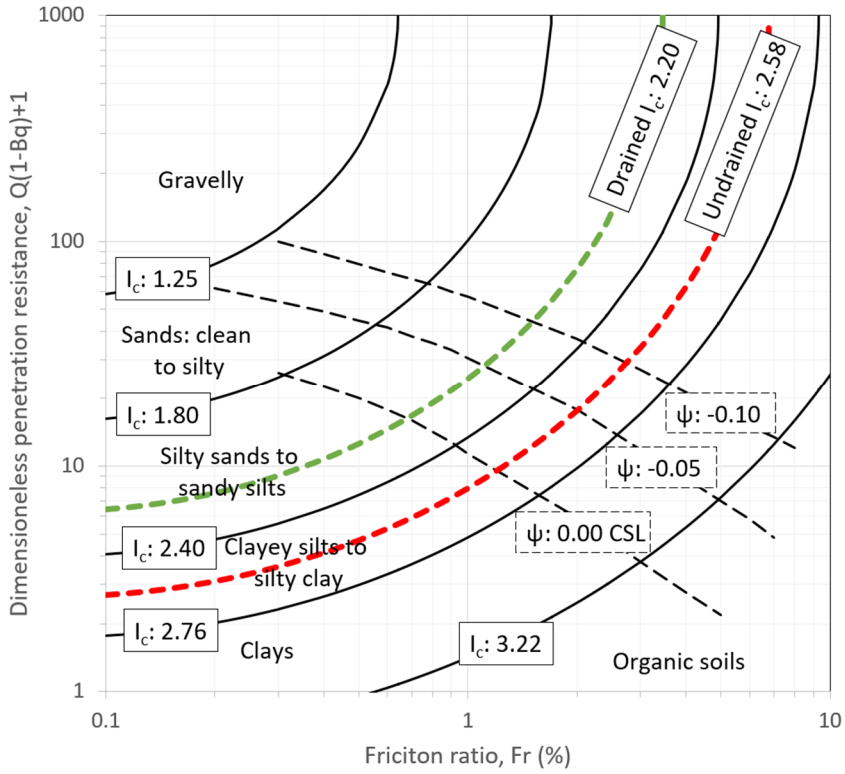

Figure 4 Soil type classification chart showing constant soil behaviour-type index contours, state parameter contours, and the assumed drained/undrained limits based on the soil behaviour-type index

$$I_c = \sqrt{\left(3 - \log\left(Q\left(1 - B_q\right) + 1\right)\right)^2 + (1.5 + 1.3 \times \log(F_r))^2} \quad (5)$$

where:

I_c = soil behaviour-type index

F_r = friction ratio.

Additionally, shown in Figure 4 are several ψ contours as well as the assumed drained/undrained I_c limits, that are within the 'silty sands to sandy silts' for the drained case (I_c=2.2), and in the 'clayey silts to silty clay' for the undrained case (I_c=2.58), as suggested by Ku et al. (2010). However, it is noted that these limits could vary depending on soil conditions, and that further research is needed to allocate these as constant values.

When using I_c = 2.2 and 2.58 for the drained and undrained limits, respectively, there is still a behavioural aspect to be reviewed, about the way drainage varies between the drained and undrained limits. As shown in Figure 5, different c values (from Equation 4) have been tested to review the variation when I_c is used to infer the drainage regime from CPT data. While the curved lines represent an approximation to the behaviour of V presented by DeJong & Randolph (2012), there is insufficient data to conclude the regime will vary to a similar extent for I_c, hence, a linear variation will be adopted for simplicity.

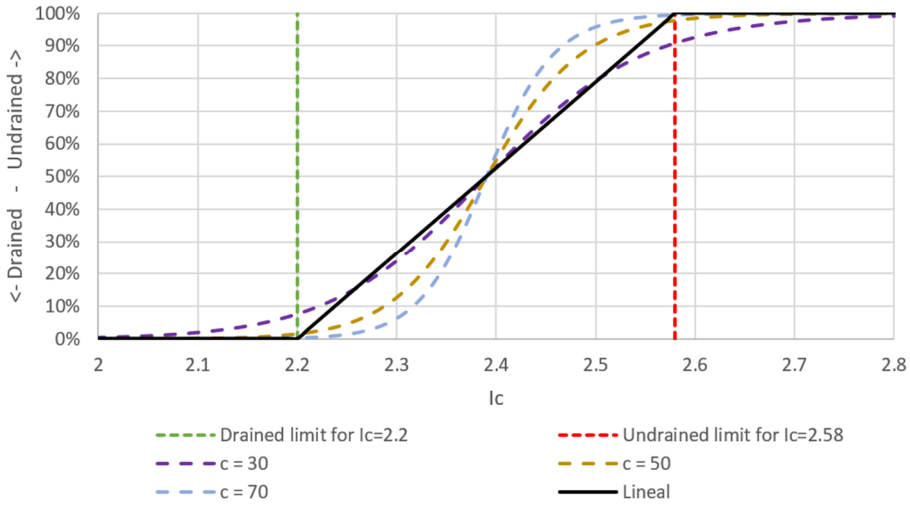

Figure 5 Different drainage variations for the soil behaviour-type index, including some with the characteristic surface approximation (c = 30, 50, and 70), and a lineal variation

The linear I_c variation shown in Figure 5 can be obtained with Equation 6:

$$\%I_c = 0\% \; for \; I_c \leq I_{cDrained} = 2.2$$

$$\%I_c = \frac{(I_c - I_{cDrained})}{(I_{cUndrained} - I_{cDrained})} \times 100\% \; for \; 2.2 > I_c > 2.58$$

$$\%I_c = 100\% \; for \; I_c \geq I_{cUndrained} = 2.58 \quad (6)$$

where:

$\%I_c$ = percentage representation of the drainage regime from the soil behaviour-type index

$I_{cDrained}$ = soil behaviour-type index limit for drained penetration

$I_{cUndrained}$ = soil behaviour-type index limit for undrained penetration.

Once the $\%I_c$ values are calculated from the CPT I_c data, the equivalent ψ can be calculated in between the drained and undrained regime trendlines, for contractive and dilative behaviour, using Equation 7:

$$\psi = \frac{-\ln\left(Q(1-B_q)+1/k_{dr}\right)}{m_{dr}} + \%I_c \times \left(\frac{-\ln\left(Q(1-B_q)+1/k_{un}\right)}{m_{un}} + \frac{\ln\left(Q(1-B_q)+1/k_{dr}\right)}{m_{dr}} \right) \quad (7)$$

4 Method review with synthetic cone penetration test data

To review the ψ inferred using the method proposed in this work, synthetic CPT $Q(1-B_q)+1$ and I_c data values were generated with known variations to illustrate the behaviour of Equations 6 and 7. $Q(1-B_q)+1$ was increased with depth from 0.1 to over 1,000, while I_c was varied with depth with zigzag values between 2.0 and 2.8, aiming to constantly move between drained and undrained responses when increasing $Q(1-B_q)+1$. As can be seen in Figure 6a, $Q(1-B_q)+1$ increases to over 1,000 at ~9.5 m depth, Figure 6b has the I_c zigzag behaviour, Figure 6c shows the percentage values calculated using Equation 6, and Figure 6d shows the equivalent ψ calculated using Equation 7.

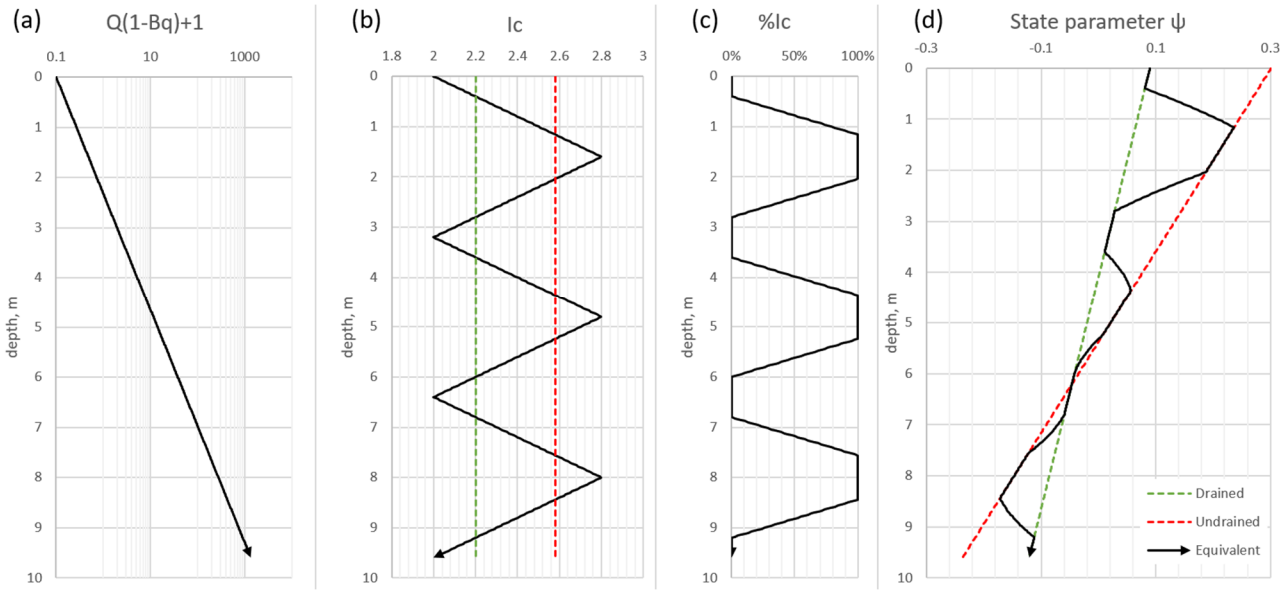

Figure 6 Synthetic cone penetration test with (a) constantly increasing normalised tip resistance with depth, (b) variable soil behaviour-type index between drained and undrained limits, (c) percentage representation of the drained and undrained responses based on the soil behaviour-type index, and (d) the inferred state parameter

As can be seen in Figure 6d, the ψ values calculated with Equations 6 and 7 vary according to the proposed method, showing negligible variations for Q(1-Bq)+1 values close to the drained-undrained crossover, and larger variations when away from the trendlines cross point. Like Figure 1, Figure 7 presents the [Q(1-Bq)+1]-ψ drained and undrained trendlines, including the equivalent ψ variation while increasing Q(1-Bq)+1 with depth, as shown in Figure 6a, for the zigzag Ic variation shown in Figure 6b.

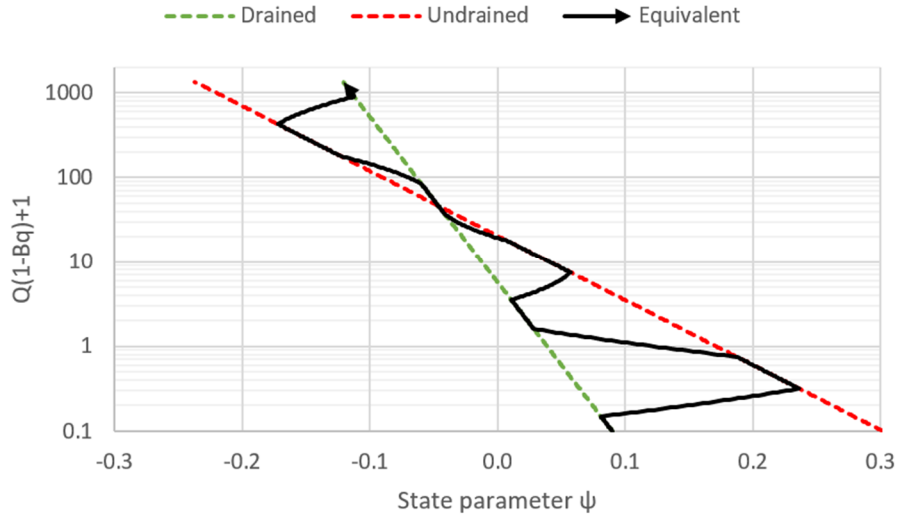

Figure 7 Normalised tip resistance correlation with the state parameter, including the equivalent drainage response for the synthetic cone penetration test, based on soil behaviour-type index

5 Other applications for this method

While this work has used the presented method for a synthetic material that responds to the CPT advance near the I_c 'partially drained zone' (e.g. thickened tailings, some silty tailings), it is worth noting that the methodology can also be applied to a soil deposit comprising two different characteristic materials, with approximated I_c limits, that have differing responses in drained (e.g. sandy tailings, some silty tailings) and undrained (e.g. clayey tailings) regimes. To illustrate this, Figure 8 presents three coloured regions where

normalised CPT data from an Australian mining project are usually concentrated. In the blue region, the upper thickened tailings fall within the previously mentioned I_c 'partially drained zone', while the yellow and orange regions are where the data of sandy and clayey tailings, respectively, are usually plotted. Now the convenience of using this method for the latter situation is, for instance, when CPT probing embankments of upstream raised TSFs and constant interaction of these two materials is usually found. Moreover, this method supports the characterisation of the interaction zones with intermediate I_c response. Hence, the implementation of this method in the CPT analysis spreadsheet, works for both scenarios.

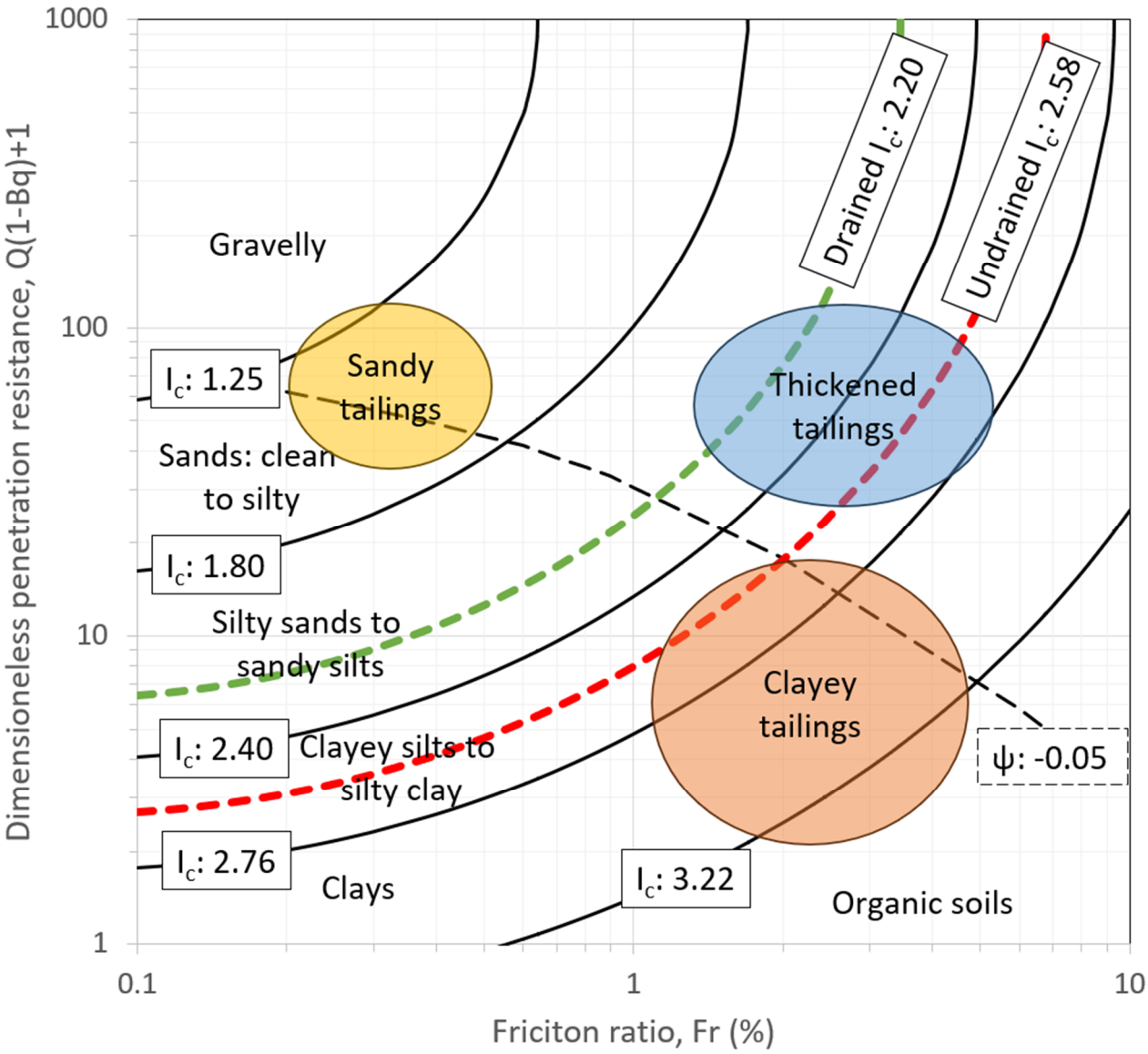

Figure 8 Soil type classification chart showing constant soil behaviour-type index contours, state parameter contours, and the assumed drained/undrained limits based in the soil behaviour-type index, in addition to regions were cone penetration test data of an Australian tailings storage facility is usually plotted

6 Paste thickened and pulp tailings drainage review

CPT data for a TSF located in Europe is presented in Figure 9, where ~2.5 m of paste thickened tailings overly subaqueously deposited pulp tailings. It is evident that even paste tailings can be in a contractive state. Additionally, for both materials, a wide range of I_c values is shown, moving several times between drained and undrained zones.

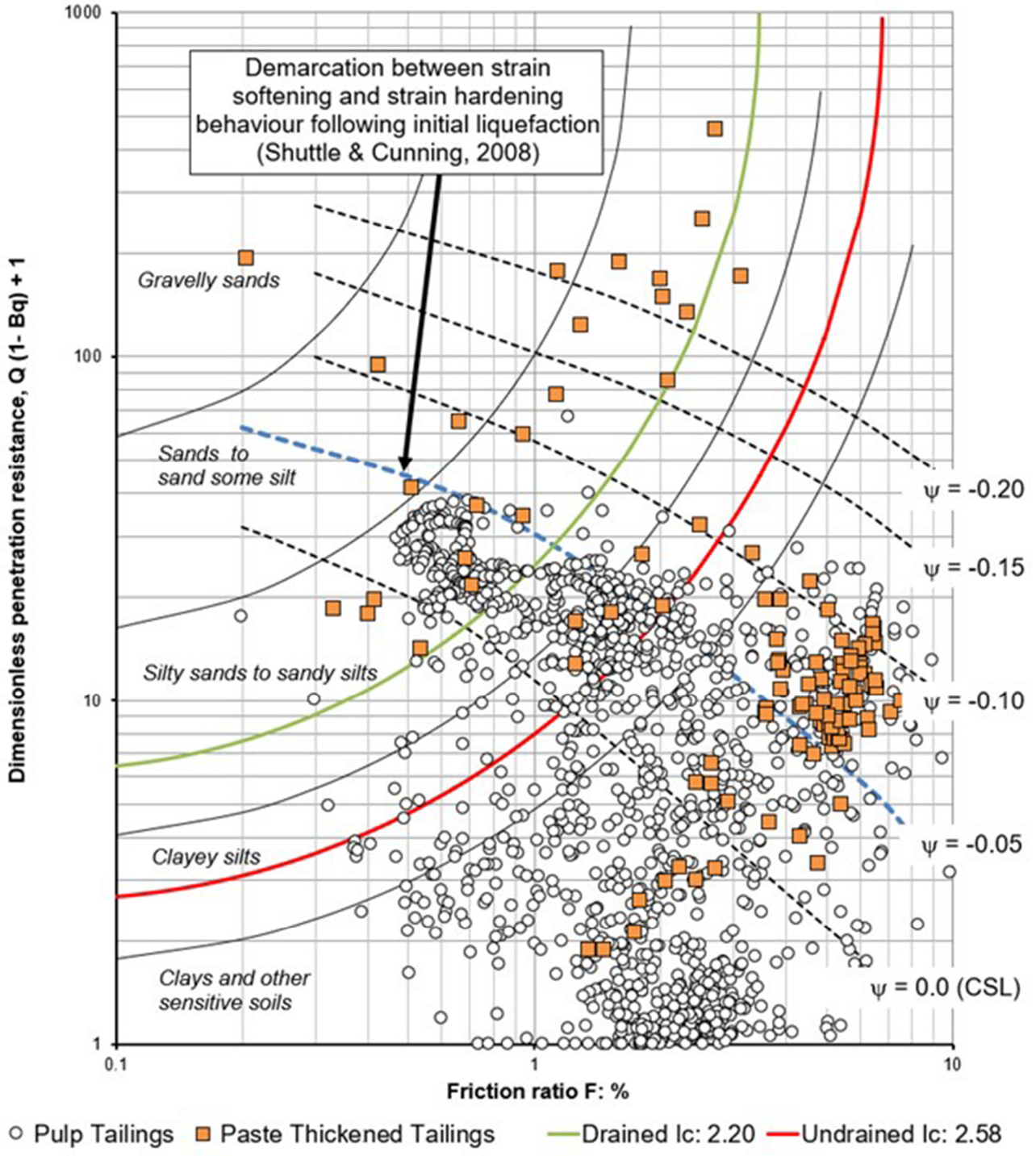

Figure 9 Mainly contractive cone penetration test data of paste thickened tailings overlying subaqueous deposited pulp tailings

By reviewing the CPT data with depth, as presented in Figure 10, the normalised tip resistance, normalised pore pressure, and soil behaviour-type index show a typical TSF scenario, where values rise and fall in accordance with the characteristics of soils with drained and undrained response to the CPT advance, as indicated in Figure 10d. The equivalent ψ varies accordingly between both drainage regimes, including some depths with values maintained in partially drained conditions, as shown in Figure 10e.

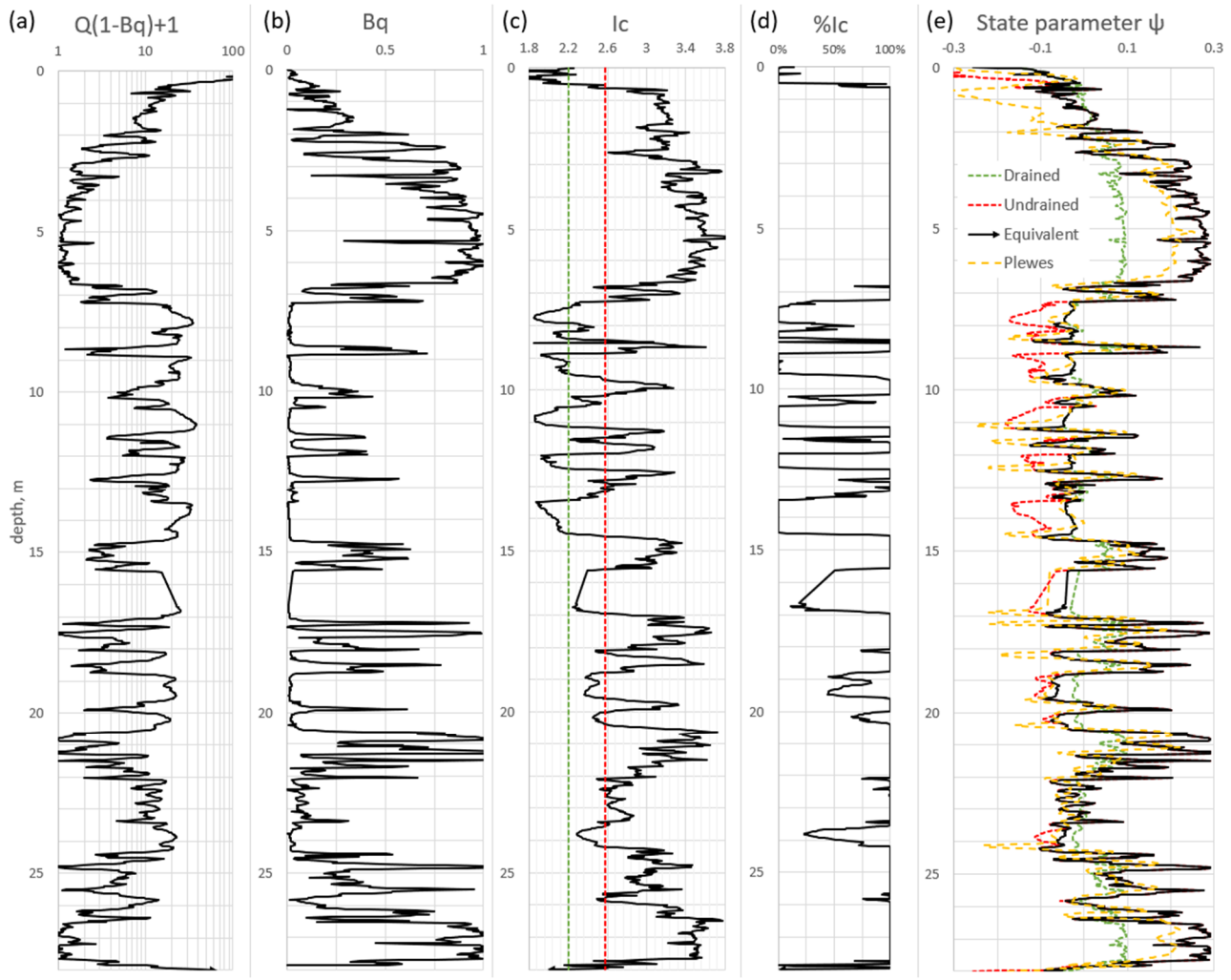

Figure 10 CPT data with (a) normalised tip resistance; (b) normalised pore pressure; (c) variable soil behaviour-type index with drained and undrained limits; (d) percentage representation of the drained and undrained response based on the soil behaviour-type index; (e) the inferred state parameters

Figure 10e also shows the results of application of the Plewes et al. (1992) method to infer the ψ. The Plewes method is often regarded as primarily being a screening level method and is thus usually considered without further reviews for adaptation to partially drained conditions. The Plewes method infers ψ values closer to the partially drained region when compared to the drained/undrained limits (e.g. between ~3 to 6 m depth), where an undrained response could be expected due to the high Bq. Moreover, it infers values outside the expected range (e.g. the dilative spikes between ~11 to 24 m depth) and infers an undrained response when Bq values are close to 0 (e.g. between ~15.5 to 17 m depth), instead of inferring a drained response in the way the method proposed in this work does.

Finally, similar to Figure 7, the CPT data presented in Figure 10 is now shown in the [Q(1-Bq)+1]-ψ space in Figure 11, where it is evident that the Plewes method infers ψ's outside of the expected drained/undrained limits. Hence, it is recommended that when the drained/undrained correlations are available, checks on the inferred response in relation to the Bq should be performed.

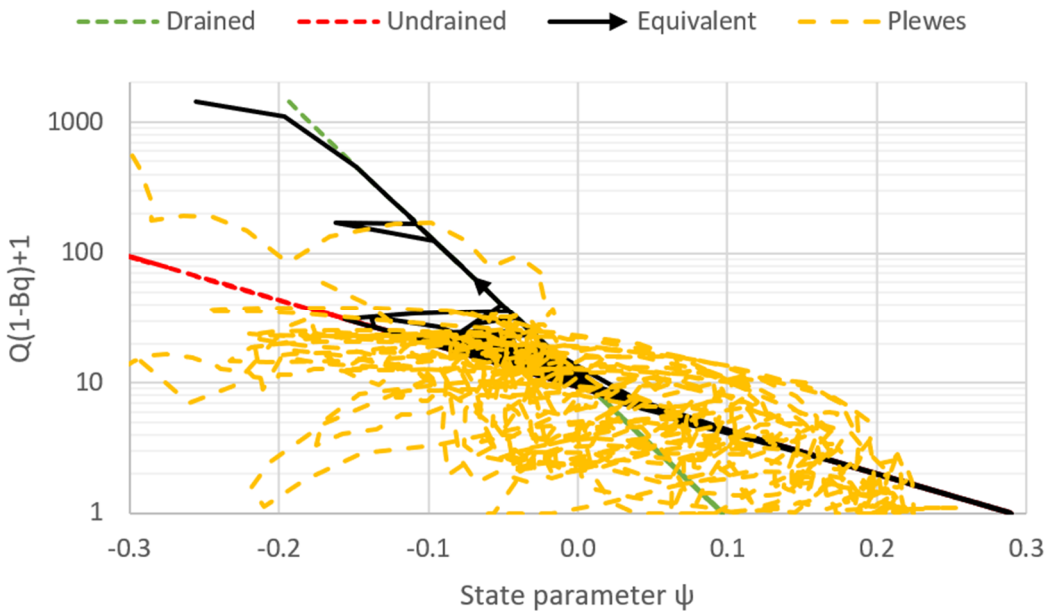

Figure 11 Normalised tip resistance correlation with the state parameter including the equivalent drainage response for the synthetic cone penetration test based on soil behaviour-type index

7 Conclusion

Based on the method described in this work and the equations presented on the use of the soil behaviour-type index to vary the normalised tip resistance-state parameter correlations, the following conclusions are drawn:

- From the normalised tip resistance-state parameter correlations, it is evident that a wide variation in the interpretation of the state parameter can result when choosing drained or undrained correlations, depending on the drainage assumption made for each probing.
- From the normalised tip resistance-state parameter drained/undrained correlations, it is evident that when the soil state parameter is near the drained-undrained crossover point, the CPT may not record excess pore pressures because negligible volumetric changes are expected near this point. This occurs even for low permeability materials, where undrained response is expected.
- Some paste thickened tailings tend to plot their soil behaviour-type index in the 'partially drained region', leading to uncertainty in the use of drained or undrained correlations to infer the state parameter. The method and equations presented in this work provide an appropriate path for these assessments.
- The common lack of knowledge of how much excess pore pressure was mobilised during a partially drained penetration, when compared to fully undrained, motivated the development of this simplified method.
- Equations to calculate the equivalent state parameter based on the soil behaviour-type index have been documented in this paper.
- When selecting the variation equation for the drainage regime based on the soil behaviour-type index, a linear variation was selected due to the lack of laboratory data or literature results that indicate otherwise.
- Application of the proposed method to two distinctly different materials typically within a tailings deposit has been used to show the versatility of the method.

- CPT data from a tailings storage facility comprising paste thickened tailings and pulp tailings were presented, and the inferred state parameters compared to those developed with the Plewes et al. (1992) method, which is commonly presumed to work in partially drained conditions. The comparison indicates that while the method presented in this work requires more data (i.e. k and m pairs), it gives more control to the engineer over the inferred values by enabling the known drained/undrained boundaries to be maintained, thereby making it an improved tool for state parameter estimation in partially drained conditions.

References

Ayala, J 2022, *Assessment of the State Parameter in Mine Tailings Using Cone Penetration Tests With Calibration Chambers*, PhD thesis, The University of Western Australia, Perth.

Ayala, J, Fourie, A & Reid, D 2023, 'A unified approach for the analysis of CPT partial drainage effects within a critical state soil mechanics framework in mine tailings', *Journal of Geotechnical and Geoenvironmental Engineering*, vol. 149, no. 6, https://doi.org/10.1061/JGGEFK.GTENG-10915

Ayala, J, Fourie, A & Reid, D 2022, 'Improved cone penetration test predictions of the state parameter of loose mine tailings', *Canadian Geotechnical Journal*, vol. 59, no. 11, https://doi.org/10.1139/cgj-2021-0460

Ayala, J, Fourie, A & Reid, D 2020, 'Cone penetration testing on silty tailings using a new small calibration chamber tailings', *Géotechnique Letters*, vol. 10, no. 4, pp. 492–497, https://doi.org/10.1680/jgele.20.00037

Been, K, Crooks, JHA, Becker, DE & Jefferies, MG 1986, 'The cone penetration test in sands: part I, state parameter interpretation', *Géotechnique*, vol. 36, no. 2, pp. 239–249, https://doi.org/10.1680/geot.1986.36.2.239

Been, K & Jefferies, MG 1992, 'Towards systematic CPT interpretation', *Predictive Soil Mechanics: The Wroth Memorial Symposium*, Oxford, pp. 121–134.

DeJong, JT & Randolph, M 2012, 'Influence of partial consolidation during cone penetration on estimated soil behavior type and pore pressure dissipation measurements', *Journal of Geotechnical and Geoenvironmental Engineering*, vol. 138, no. 7, pp. 777–788, https://doi.org/10.1061/(ASCE)GT.1943-5606.0000646

Dienstmann, G, Schnaid, F, Maghous, S & DeJong, J 2018, 'Piezocone penetration rate effects in transient gold tailings', *Journal of Geotechnical and Geoenvironmental Engineering*, vol. 144, no. 2, https://doi.org/10.1061/(ASCE)GT.1943-5606.0001822

Finnie, IMS & Randolph, MF 1994, 'Punch-through and liquefaction induced failure of shallow foundations on calcareous sediments', *Proceedings of the 7th International Conference on Behavior of Offshore Structures*, Boston, vol. 1, pp. 217–230.

Ghafghazi, M & Shuttle, D 2008, 'Interpretation of sand state from cone penetration resistance', *Géotechnique*, vol. 58, no. 8, pp. 623–634, https://doi.org/10.1680/geot.2008.58.8.623

Houlsby, GT 1988, 'Discussion session contribution', *Penetration Testing in the UK*, Institution of Civil Engineers, Birmingham.

House, AR, Oliveira, JRMS & Randolph, MF 2001, 'Evaluating the coefficient of consolidation using penetration tests', *International Journal of Physical Modelling in Geotechnics*, vol. 1, no. 3, pp. 17–26, https://doi.org/10.1680/ijpmg.2001.010302

Jaeger, RA, DeJong, JT, Boulanger, RW, Low, HE & Randolph, MF 2010, 'Variable penetration rate CPT in an intermediate soil', *Proceedings of the 2nd International Symposium on Cone Penetration Testing*, Huntington Beach.

Jefferies, MG & Been, K 2015, 'Soil liquefaction: a critical state approach', 2nd edn, *Applied Geotechnics Series*, CRC Press, Boca Raton.

Ku, CS, Juang, CH & Ou, CY 2010, 'Reliability of CPT Ic as an index for mechanical behaviour classification of soils', *Géotechnique*, vol. 60, no. 11, pp. 861–875, https://doi.org/10.1680/geot.09.P.097

Lehane, BM, O'Loughlin, CD, Gaudin, C & Randolph, MF 2009, 'Rate effects on penetrometer resistance in kaolin', *Géotechnique*, vol. 59, no. 1, pp. 41–52, https://doi.org/10.1680/geot.2007.00072

Low, HE, Randolph, MF, Lunne, T, Andersen, KH & Sjursen, MA 2011, 'Effect of soil characteristics on relative values of piezocone, T-bar and ball penetration resistances', *Géotechnique*, vol. 61, no. 8, pp. 651–664, https://doi.org/10.1680/geot.9.P.018

Mahmoodzadeh, H & Randolph, MF 2014, 'Penetrometer testing: effect of partial consolidation on subsequent dissipation response', *Journal of Geotechnical and Geoenvironmental Engineering*, vol. 140, no. 6, https://doi.org/10.1061/(ASCE)GT.1943-5606.0001114

Mahmoodzadeh, H, Randolph, MF & Wang, D 2014, 'Numerical simulation of piezocone dissipation test in clays', *Géotechnique*, vol. 64, no. 8, pp. 657–666, https://doi.org/10.1680/geot.14.P.011

Plewes, HD, Davies, MP & Jefferies, MG 1992, 'CPT based screening procedure for evaluation liquefaction susceptibility', *45th Canadian Geotechnical Conference,* Canadian Geotechnical Society, Toronto, pp. 41–49.

Randolph, MF & Hope, SF 2004, 'Effect of cone velocity on cone resistance and excess pore pressures', *Proceedings of the IS Osaka International Symposium on Engineering Practice and Performance of Soft Deposits*, Yodogawa Kogisha Co Ltd, Osaka, vol. 1, pp. 147–152.

Reid, D 2015, 'Estimating slope of critical state line from cone penetration test — an update', *Canadian Geotechnical Journal*, vol. 52, no. 1, pp. 46–57, https://doi.org/10.1139/cgj-2014-0068

Reid, D & Fourie, AB 2018, 'Characterization of a gold tailings with hypersaline pore fluid', *Canadian Geotechnical Journal*, vol. 57, no. 4, https://doi.org/10.1139/cgj-2018-0579

Shuttle, D & Jefferies, M 2016, 'Determining silt state from CPTu', *Geotechnical Research*, vol. 3, no. 3, pp. 90–118, https://doi.org/10.1680/jgere.16.00008

Shuttle, D & Jefferies, M 1998, 'Dimensionless and unbiased CPT interpretation in sand', I*nternational Journal for Numerical and Analytical Methods in Geomechanics*, vol. 22, no. 5, pp. 351–391, https://doi.org/10.1002/(SICI)1096-9853(199805)22:5<351::AID-NAG921>3.0.CO;2-8

Shuttle, DA & Cunning, J 2008, 'Reply to the discussion by Robertson on "Liquefaction potential of silts from CPTu"', Canadian Geotechnical Journal, vol. 45, no. 1, pp. 140–141, https://doi.org/10.1139/T07-119

Shuttle, DA & Cunning, J 2007, 'Liquefaction potential of silts from CPTu', *Canadian Geotechnical Journal*, vol. 44, no. 1, pp. 1–19, https://doi.org/10.1139/t06-086

Silva, MF & Bolton, MD 2005, 'Interpretation of centrifuge piezocone tests in dilatant, low plasticity silts', I*nternational Conference on Problematic Soils (GEOPROB 2005)*, Eastern Mediterranean Universoty, Famagusta, vol. 1, pp 1–8.

Suzuki, Y & Lehane, BM, 2015, 'Cone penetration at variable rates in kaolin–sand mixtures', *International Journal of Physical Modelling in Geotechnics*, vol. 15, no. 4, pp. 209–219, https://doi.org/10.1680/ijpmg.14.00043

Yi, JT, Goh, SH, Lee, FH & Randolph, MF 2012, 'A numerical study of cone penetration in fine-grained soils allowing for consolidation effects', *Géotechnique*, vol. 62, no. 8, pp. 707–719, https://doi.org/10.1680/geot.8.P.155